Novel Frequency-Efficient Communication-Positioning Integrated Signal and Ranging Methodology for Future Aviation

Tianzhu Song, *Student Member, IEEE,* Lu Yin, *Member, IEEE,* Deming Zhu, Yuan Sun, Qiang Ni, *Senior Member, IEEE*

***Abstract*—The future of aviation is characterized by the fusion of digital technologies, data-driven decision-making, and seamless connectivity. Accurate and reliable positioning plays a pivotal role in the future aviation technologies such as autonomous flight, advanced air traffic management (ATM) systems, and augmented reality (AR) for pilot assistance. In case of global navigation satellite system (GNSS) failure, the alternative positioning, navigation, and timing (APNT) system is needed. Current methods for aviation positioning either lack the accuracy, reliability or the capacity for future air traffic development because their signal designs are outdated or not optimal for positioning. To tackle this problem, a novel communication-positioning integrated signal is designed. A continuous positioning signal is superposed onto the L-band digital aeronautical communication system (L-DACS) signal using non-orthogonal multiple access (NOMA) principle to fully utilize the frequency resources and minimize its interference to communication. A novel cross channel measuring (CCM) algorithm is proposed to measure pseudorange when the positioning signal is spread across multiple L-DACS1 channels for improved ranging accuracy. Simulation results show the novel communication-positioning integrated signal and its measuring method outperforms the existing L-DACS1 method, almost achieving meter-level ranging accuracy. And the positioning signal causes minimal interference to communication.**

***Index Terms*—Aircraft, communication-positioning integrated signal, NOMA, L-band**

I. Introduction

In the era of rapid technological advancement, civil aviation industry finds itself at the crossroads of innovation and transformation. The future of aviation is characterized by the fusion of digital technologies, data-driven decision-making, and seamless connectivity [1], [2]. As technological advancements reshape aviation, accurate positioning plays a pivotal role. Although global navigation satellite systems (GNSS) can provide high-accuracy positioning results, it is vulnerable to disruptions caused by intended or unintended radio interferences and its positioning accuracy can degenerate significantly if one or several satellites fail. Therefore, the alternative positioning, navigation, and timing (APNT) system is required [3]. Common APNT candidates include distance measuring equipment (DME), wide area multilateration (WAM), L-band digital aeronautical communication system (L-DACS), etc [4]. However, as DME uses pulse pairs to measure distance, its signal can easily be lost and suffers heavily from multipath, which results in low positioning accuracy and reliability [5]. WAM also has signal detection problem because the 1090-MHz band that it uses has been congested by various aircraft and systems [6]. In addition, technologies like DME and WAM contain both forward and backward communication links, which require the systems to work in active mode. This is not optimal in the context of rapid air traffic growth because its capacity is limited [7]. L-DACS is a communication system designed to support the higher bandwidths needed in the future for air-to-ground communications [8]. With some necessary adjustments, the candidate 1 (L-DACS1) can also be used for navigation utilizing its synchronization symbols [9]. However, since L-DACS1 signal was not designed with positioning in mind, its measuring frequency is low and the bandwidth allocated for positioning is limited [10].

The current methods for aviation positioning either lack the accuracy, reliability or the capacity for future air traffic development because their signal designs are outdated or not optimal for positioning. To meet such demand in the future landscape of aviation, a signal dedicated to positioning while causing little interference to other systems is required. In this letter, we propose a novel signal and its ranging methodology to satisfy the needs for future aviation technologies.

II. Novel communication-positioning integrated signal

A. L-DACS1 system

L-DACS1 is a cellular system that is based on a network of ground stations (GS) to provide communications services between the aircraft and the air traffic controllers. It employs orthogonal frequency division multiplexing (OFDM) for communication. As shown in Fig.1, to implement L-DACS1 into the current already congested L-band, it is employed as an inlay system between two adjacent DME channels, spectrally separated by 1 MHz. This design allows L-DACS1 to effectively utilize of frequency gaps between adjacent DME channels, minimizing its interference to other existing L-band systems.

As mentioned earlier, with some necessary adjustments, L-DACS1 can offer forward link ranging capabilities using its

This research was supported in part by the Key Research and Development Program of China under Grant 2022YFB3904502, and in part by the Beijing Municipal Natural Science Foundation under Grant 4242045. (Corresponding author: Lu Yin.)

Tianzhu Song, Lu Yin, Deming Zhu, Yuan Sun are with the School of Electronic Engineering, Beijing University of Posts and Telecommunications, Beijing, 100876, China, e-mail: stztc112358@bupt.edu.cn, inlu_mail@bupt.edu.cn, dmzhu@bupt.edu.cn, sunyuan@bupt.edu.cn

Qiang Ni is with the School of Computing and Communications, Lancaster University, InfoLab21, LA1 4WA, U.K. e-mail: q.ni@lancaster.ac.uk

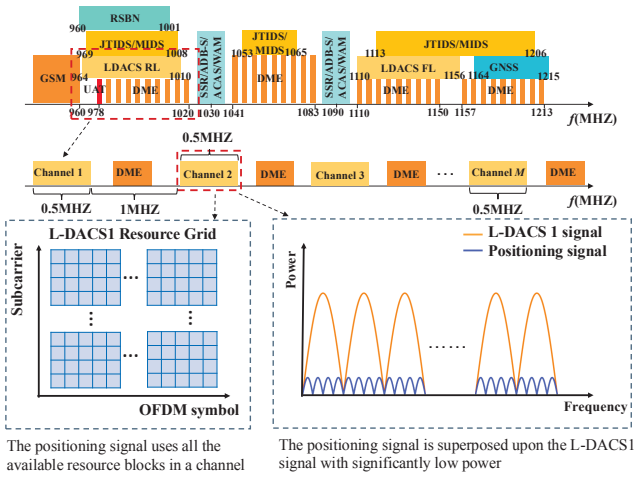

Fig. 1. Novel communication-positioning integrated signal architecture.

synchronization symbols [9]. However, due to the inlay-system nature of L-DACS1, the bandwidth for each channel is limited to 0.5MHz. In addition, because the ranging process uses only the synchronization symbols in the broadcast frame, the bandwidth allocated for positioning is even less. And the measurement can only be conducted every few seconds, which further limits its performance. Therefore, in this letter, a novel positioning-dedicated signal is designed to achieve better ranging accuracy.

B. Positioning signal and integration

The positioning signal mainly consists of pseudorandom codes and navigation messages. Pseudorandom codes are employed for the purpose of spreading gains and measuring ability. To ensure the positioning signal's compatibility with the existing aerial systems, it is integrated with L-DACS1, sharing the same frequency resources. As shown in Fig. 1, it is superposed upon each L-DACS1 channel with significantly low power using non-orthogonal multiple access (NOMA) principle to mitigate its interference to communication [11]. In addition, to improve its compatibility, it uses similar OFDM modulation configurations to L-DACS1 and share the same resource grid.

Define P_{com} and P_{pos} as the power of L-DACS1 communication signal and the positioning signal, respectively. To better represent the power relationship between the two in further analysis, define positioning-communication-ratio (PCR) as :

$$PCR = \frac{P_{pos}}{P_{com}}. \tag{1}$$

Because the positioning signal is modulated with pseudorandom codes, its low cross-correlation feature makes it shows similar properties as noise to L-DACS1. Denote the single-sided power spectral density (PSD) of the environment noise as N_0, and the bandwidth for each L-DACS1 channel as B_0, the equivalent SNR of L-DACS1 can be expressed as:

$$ESNR = \frac{SNR}{SNR \times PCR + 1}. \tag{2}$$

L-DACS1 has three modulation schemes: QPSK, 16-QAM and 64-QAM [12]. Define Γ and γ who are determined by the modulation and coding schemes, and the bit error rate (BER) degradation of L-DACS1 can be expressed as:

$$\Delta BER = \Gamma\left[erfc\left(\sqrt{\gamma ESNR}\right) - erfc\left(\sqrt{\gamma SNR}\right)\right] \tag{3}$$

$$= \Gamma[erfc\left(\sqrt{\frac{\gamma SNR}{SNR \times PCR + 1}}\right) - erfc\left(\sqrt{\gamma SNR}\right)]. \tag{4}$$

Due to the very low power of positioning signal, PCR is very small. Therefore, As (4) describes, under common SNR conditions, the BER degradation is very small. Furthermore, in certain scenarios where the BER requirements are extreme, serial interference cancellation (SIC) method [13] can be adapted to fully remove the interference of the positioning signal.

Because L-DACS1 can handle the information transmission, navigation messages are not necessary for the positioning signal. The positioning signal is able to utilize all the available L-DACS1 resources blocks without the need to reserve subcarriers. This allows the positioning signal to have larger bandwidth and enables its continuous ranging capability. As the available spectrum resources are separated by frequency gaps, the bandwidth for each channel is limited. However, due to the broadcast nature of positioning signal, it can utilize multiple L-DACS1 channels for larger bandwidth, improving its ranging performance. To employ the positioning signals across multiple L-DACS1 channels, the pseudorandom codes will be split and mapped to different channel's resource grid. As shown in Fig. 2, assume a total amount of M channels are used by the positioning signal, and the pseudorandom codes can be sequentially divided into M parts based on modulation parameters:

$$R = [R_1, R_2, ..., R_M], \tag{5}$$

where R_m represents the m-th part of R. Each part is mapped onto the resource grid of each channel in sequence to maintain the periodicity of the pseudocode across multiple channels. Then, different channels are transmitted independently with different center frequencies. The measuring method for this type of positioning signal will be introduced in the following sub-section.

C. Cross channel measuring algorithm

In order to accurately measure the distance between BS and the receiver using the proposed integrated signal, the novel CCM algorithm is proposed, and the measuring loop based on CCM is designed.

The structure of the CCM-based measuring loop for the novel signal is shown in Fig. 3. The red part highlights how the CCM algorithm is implemented. Because different L-DACS1 channels already use separate center frequencies for transmission, the receiver is able to process different signal channels

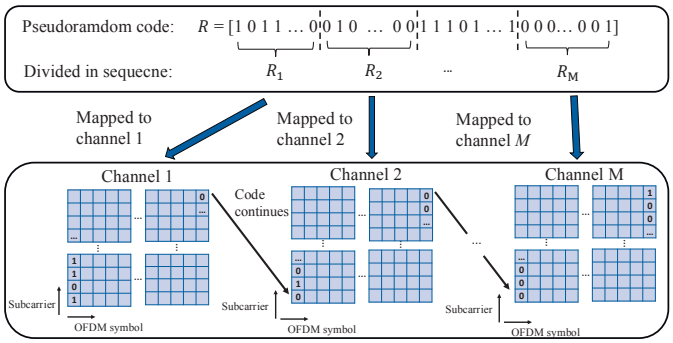

Fig. 2. Cross channel positioning resource mapping.

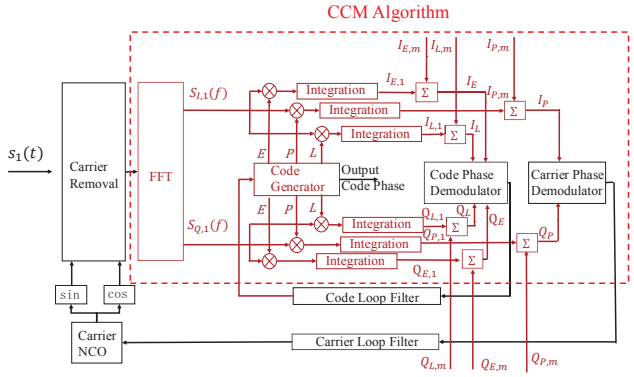

Fig. 3. The structure of the CCM-based measuring loop. The red part highlights how the CCM algorithm is implemented.

independently. Denote $R(\phi)$ and $R_m(\phi)$ as the pseudorandom codes in phase, the intermediate frequency signal input can be expressed as:

$$s_m(t) = A_{IF} e^{j\theta(t)} \sum_{n=0}^{N-1} R_m\left(\frac{n\Phi}{MN}\right) e^{j2\pi n\Delta f t}. \quad (6)$$

A_{IF} is the intermediate frequency amplitude. $\theta(t)$ is the carrier phase at t. N is the total number of used sub-carrier in one channel. Φ is the total phase of pseudorandom code. Δf is the sub-carrier spacing. Denote τ as propagation delay, after carrier removal and OFDM demodulation, (6) becomes:

$$S_m(f,\tau) = A_{IF} e^{j\Delta\theta} \sum_{n=0}^{N-1} R_m(\frac{n\Phi}{MN}) e^{-j2\pi n\Delta f\tau} \delta(f - n\Delta f), \quad (7)$$

where $\Delta\theta$ is the residual carrier phase. Define $\widetilde{R}_m(f,\tau)$ to simplify the expression of Equation (7):

$$\widetilde{R}_m(f,\tau) = \sum_{n=0}^{N-1} R_m(\frac{n\Phi}{MN}) e^{-j2\pi n\Delta f\tau} \delta(f - n\Delta f). \quad (8)$$

And (7) can be expressed as:

$$S_m(f,\tau) = A_{IF} e^{j\Delta\theta} \widetilde{R}_m(f,\tau) \quad (9)$$

$$= S_{I,m}(f,\tau) + jS_{Q,m}(f,\tau), \quad (10)$$

where $S_{I,m}(f,\tau)$ represent the I channel input, and $S_{Q,m}(f,\tau)$ for the Q channel.

To measure the code phase of the received signal, the local pseudorandom codes from the code generator are correlated with $S_{I,m}(f,\tau)$ and $S_{Q,m}(f,\tau)$. Note that early code, prompt code and late code expressions are similar but with different local code phase. For analytical convenience, prompt code is used in the following discussions. Denote ς as the local code phase in time, the local prompt code output from the code generator can be expressed as:

$$C_{P,m}(f,\varsigma) = \sum_{n=0}^{N-1} R_m(\frac{n\Phi}{MN}) e^{-j2\pi n\Delta f\varsigma} \delta(f - n\Delta f). \quad (11)$$

Therefore, the local integration process for the prompt code is expressed as:

$$I_{P,m} = A_{IF} sin\Delta\theta \int_0^{(N-1)\Delta f} \widetilde{R}_m(f,\tau) C^*_{P,m}(f,\varsigma)\, df, \quad (12)$$

$$Q_{P,m} = A_{IF} cos\Delta\theta \int_0^{(N-1)\Delta f} \widetilde{R}_m(f,\tau) C^*_{P,m}(f,\varsigma)\, df. \quad (13)$$

When only one frequency channel is used, due to the properties of pseudorandom codes, the correlation result between the received code and local code will peak when $\varsigma = \tau$. The correlation result $V_P(\varsigma)$ can be expressed as:

$$V_P(\varsigma) = \int_0^{M(N-1)\Delta f} \widetilde{R}(f,\tau) C^*_P(f,\varsigma)\, df, \quad (14)$$

where $C_P(f,\varsigma)$ is the code generator output when the code is not spitted in the way of Fig. 2. Based on the mapping process in Fig. 2, (14) can be further derived as follows:

$$V_P(\varsigma) = \int_0^{(N-1)\Delta f} \widetilde{R}(f,\tau) C^*_P(f,\varsigma)\, df + ... + \int_{(M-1)(N-1)\Delta f}^{M(N-1)\Delta f} \widetilde{R}(f,\tau) C^*_P(f,\varsigma)\, df \quad (15)$$

$$= \Sigma_{m=1}^{M} \int_{(m-1)(N-1)\Delta f}^{m(N-1)\Delta f} \widetilde{R}(f,\tau) C^*_P(f,\varsigma)\, df \quad (16)$$

$$= \Sigma_{m=1}^{M} \int_0^{(N-1)\Delta f} \widetilde{R}_m(f,\tau) C^*_{P,m}(f,\varsigma)\, df. \quad (17)$$

This means that the correlation properties of the pseudorandom code is still maintained after the mapping process in Fig. 2. Therefore, for multiple separated positioning channels, the integration process in (12) and (13) can be conducted individually for each channel and summed up:

$$I_P = \Sigma_{m=1}^{M} I_{P,m}, \quad (18)$$

$$Q_P = \Sigma_{m=1}^{M} Q_{P,m}. \quad (19)$$

And $V_P(\varsigma)$ can be calculated with:

$$V_P(\varsigma) = \frac{1}{A_{IF}} \sqrt{I_P^2 + Q_P^2}. \quad (20)$$

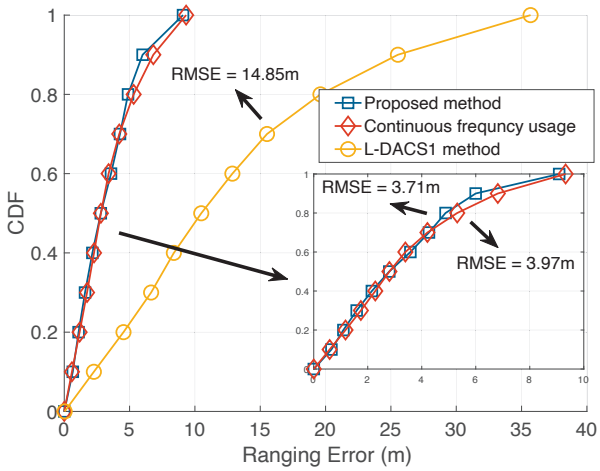

Fig. 4. The ranging error cumulative distribution functions (CDF) comparison between the proposed method, positioning signal occupying continuous frequency resource and the L-DACS1 method. (Positioning bandwidth B = 2MHz, PCR=-20dB, communication SNR =10dB)

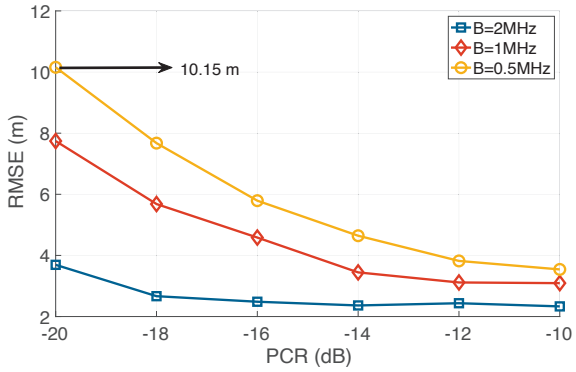

Fig. 5. The ranging RMSEs of the proposed method under different PCR and different bandwidths. (Communication SNR =10dB)

After calculating the correlation result of early, prompt and late code using (18)-(20), traditional code/carrier phase demodulator and loop filter from [14] are used to calculate and adjust the local phase to better track the signal. The code phase output from the local code generator can be used as the ranging result in further positioning calculations.

III. Performance Evaluation

In this section, the performance of proposed signal and the CCM algorithm is evaluated through simulations. The L-DACS1 setup for ranging accuracy analysis is based on [9], using QPSK. To better evaluate the robustness of the proposed method, an air to ground multipath channel model based on [15] is used (with a Rican factor $K = 10$). For each scenario, simulation is conducted with Monte Carlo method for 50 runs. Note that the accuracies of DME and WAM are typically in the range of tens of meters at best [16], [17], and the proposed method aims to offer close-to-meter-level accuracy. Therefore, the newer, more advanced L-DACS1 ranging method introduced in [9] is used as benchmark for performance analysis.

The benchmark method employs a frequency-domain correlation mechanism. It compares two received signal sequences in different windows, with a complexity of $O(N)$. The proposed method tracks the phase of the signal in frequency domain, which involves coherent integration and phase discrimination to adjust the phase of local codes in each instance, leading to a complexity of $O(N)$. Both methods require FFT operations with a complexity of $O(N \log N)$ to operate in frequency domain. As the FFT process accounts for the majority of computation, the computational complexity of the two methods are similar.

Fig. 4 shows the CDF comparison between the proposed method, positioning signal occupying continuous frequency resource and the L-DACS1 method. The root mean squared error (RMSE) of the proposed method is only 3.71m, which is an 75% accuracy improvement to the existing L-DACS1 method. This shows that the proposed method is able to significantly increase the ranging accuracy by utilizing multiple frequency channels. In addition, it is observed that the curve of continuous frequency usage is very close to the proposed method, and the RMSEs difference between of them are also very small. Positioning signal occupying continuous frequency resource refers to the theoretical scenario where the positioning signal's frequency usage is not limited by the discrete aerial spectrum. This indicates that with the proposed CCM algorithm, the cross-channel positioning signal is able to maintain its performance regarding common positioning signal using the same bandwidth. Also notice that the PCR in Fig. 4 is only -20dB, which can be further increased for better ranging accuracy.

Fig. 5 shows the ranging RMSE of the proposed method under different PCR and different bandwidths. It is obvious that the ranging accuracy improves with higher PCR and bandwidth. Note that even when the proposed method uses only 0.5MHz bandwidth for positioning, its ranging accuracy almost reaches meter-level (10.15 m), which already outperforms the existing L-DACS1 ranging method by 31.6% without utilizing multiple channels. In addition, notice that the accuracy improvement brought by the additional bandwidth is more significant under lower PCR. This is because the positioning signal with larger bandwidth (i.e. more channels utilized) uses longer pseudorandom codes, which has better correlation properties, leading to more robust ranging capabilities. Fig. 5 also shows that with the appropriate bandwidth and PCR, the proposed methodology can almost achieve submeter level ranging accuracy.

Fig. 6 evaluates the interference of the positioning signal to L-DACS1 communication signal with BER. It shows that in common SNR range for airplanes (i.e. between 0dB and 10dB [9]), the curves with different PCRs are very close to the one where $PCR = -\infty$dB (i.e. no positioning signal). This means that with the appropriate PCR, the positioning signal causes little interference to L-DACS1 communication signal. It can also be observed that as SNR gets higher, the BER degradation becomes more severe. This is because in more ideal scenarios for communication, the interference caused by the positioning signal will become more dominant regarding

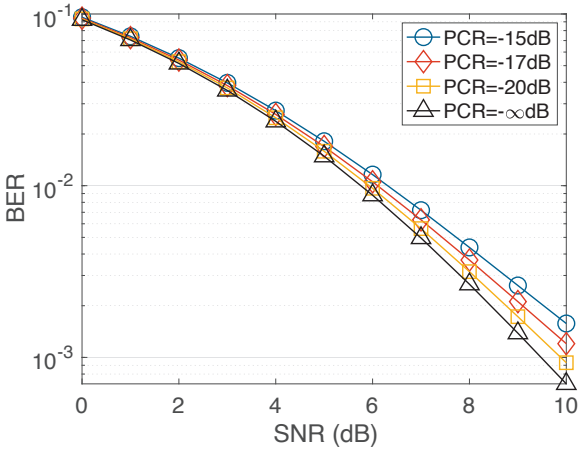

Fig. 6. The L-DACS1 BER with different PCRs under different SNRs. (QPSK modulation)

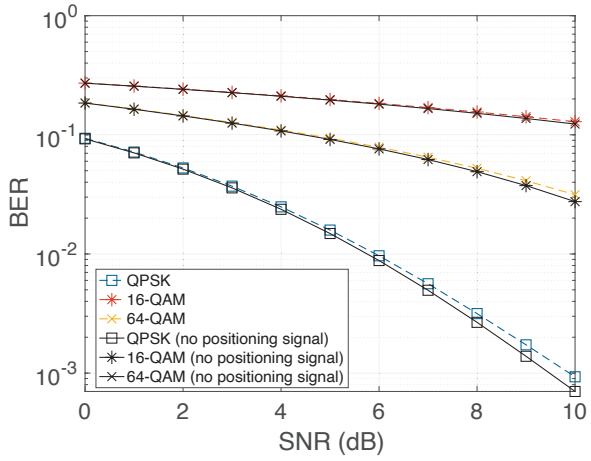

Fig. 7. The L-DACS1 BER using different modulation scheme. (PCR =-20dB)

to environment noise.

Fig. 7 shows the BER performance of L-DACS1 using QPSK, 16-QAM and 64-QAM when integrated with the positioning signal. The BER performance of L-DACS1 without the superposed positioning signal is used as reference. It can be seen that for all three modulation order, there are little the BER degradation. It can also be seen that although 64-QAM modulation order is theoretically the most sensitive to external interference, the BER degradation is the least significant. This is because the power of the superposed signal is so low that the main contributing factor of BER degradation is still the environmental noise and multipath rather than positioning signal. This further shows how the interference caused by positioning signal is incremental.

IV. Conclusion

In this letter, a novel communication-positioning integrated signal and its measuring method is designed to provide high level ranging accuracy for future aviation. The positioning component can utilize multiple fragmented communication channels for larger bandwidth to significantly increase its ranging accuracy. To measure the novel signal, a new method called cross channel measuring algorithm and its measuring loop is designed. Simulation results show that the novel signal significantly outperforms the existing L-DACS1 method. And the positioning signal causes little interference to communication.

References

[1] J. Sekera and A. Novak, "The future of data communication in aviation 4.0 environment," *Incas Bulletin*, vol. 13, no. 3, pp. 165–178, 2021.

[2] R. A. Valdés, V. F. G. Comendador, A. R. Sanz, and J. P. Castán, "Aviation 4.0: more safety through automation and digitization," in *Aircraft technology*. IntechOpen, 2018.

[3] B. W. Parkinson, Y. J. Morton, F. van Diggelen, and J. J. Spilker Jr, "Introduction, early history, and assuring PNT (PTA)," *Position, Navigation, and Timing Technologies in the 21st Century: Integrated Satellite Navigation, Sensor Systems, and Civil Applications*, vol. 1, pp. 1–42, 2020.

[4] D. Lawrence, "Alternative positioning, navigation, and timing (APNT)," *13th National Space-based PNT Advisory Board*, vol. 1, no. 1, pp. 1–26, 2014.

[5] M. Narins, L. Eldredge, P. Enge, M. Harrison, R. Kenagy, and S. Lo, "Alternative position, navigation, and timing–the need for robust radionavigation," in *Global Navigation Satellite Systems: Report of a Joint Workshop of the National Academy of Engineering and the Chinese Academy of Engineering*. The National Academies Press Washington, DC, USA, 2012, pp. 119–136.

[6] S.-L. Jheng and S.-S. Jan, "Implementation of wide area multilateration using a 1090 MHz ADS-B signal," *Journal of Aeronautics, Astronautics and Aviation*, vol. 53, no. 1, pp. 13–25, 2021.

[7] S. Han, Z. Gong, W. Meng, C. Li, and X. Gu, "Future alternative positioning, navigation, and timing techniques: A survey," *IEEE wireless communications*, vol. 23, no. 6, pp. 154–160, 2016.

[8] D. Wang, S. Wu, Y. Gao, and L. Sang, "Research on iterative receiving algorithm for aviation communication system," in *2020 IEEE 19th International Conference on Cognitive Informatics & Cognitive Computing (ICCI*CC)*. IEEE, 2020, pp. 162–168.

[9] N. Schneckenburger, D. Shutin, and M. Schnell, "Precise aeronautical ground based navigation using LDACS1," in *2012 Integrated Communications, Navigation and Surveillance Conference*, 2012, pp. B1–1–B1–10.

[10] N. Schneckenburger, B. Elwischger, B. Belabbas, D. Shutin, M.-S. Circiu, M. Suess, M. Schnell, J. Furthner, and M. Meurer, "Navigation performance using the aeronautical communication system LDACS1 by flight trials," in *European Navigation Conference*, April 2013. [Online]. Available: https://elib.dlr.de/81532/

[11] L. Yin, J. Cao, Q. Ni, Y. Ma, and S. Li, "Design and performance analysis of multi-scale noma for future communication-positioning integration system," *IEEE Journal on Selected Areas in Communications*, vol. 40, no. 4, pp. 1333–1345, 2022.

[12] T. Gräupl, C. Rihacek, B. Haindl, and Q. Parrod, "PJ.14-W2-60 TRL6 final LDACS A/G specification," in *Ed. 01.00.00, SESAR-IR-VLD-WAVE2-12-2019*, 2023.

[13] H. Li, W. He, Q. He, and J. He, "The application and development of SIC technology in wireless communication system," in *2017 IEEE 9th International Conference on Communication Software and Networks (ICCSN)*. IEEE, 2017, pp. 565–570.

[14] R. Yang, X. Zhan, W. Chen, and Y. Li, "An iterative filter for FLL-assisted-PLL carrier tracking at low C/N0 and high dynamic conditions," *IEEE Transactions on Aerospace and Electronic Systems*, vol. 58, no. 1, pp. 275–289, 2022.

[15] J. H. Bae, Y. S. Kim, N. Hur, and H. M. Kim, "Study on air-to-ground multipath channel and mobility influences in uav based broadcasting," in *2018 International Conference on Information and Communication Technology Convergence (ICTC)*, 2018, pp. 1534–1538.

[16] I. Ostroumov and N. Kuzmenko, "Performance of vor/dme navigation aided by altimeter data," in *2022 12th International Conference on Advanced Computer Information Technologies (ACIT)*, 2022, pp. 428–431.

[17] S.-L. Jheng, S.-S. Jan, Y.-H. Chen, and S. Lo, "1090 MHz ADS-B-based wide area multilateration system for alternative positioning navigation and timing," *IEEE Sensors Journal*, vol. 20, no. 16, pp. 9490–9501, 2020.